© 2014 IJEDR | Volume 2, Issue 4 | ISSN: 2321-9939

Design and Geometrical Analysis of Propellant Grain Configurations of a Solid Rocket Motor

[1]Patan Stalin, [2]Y.N.V.Santosh Kumar, [3]SK.Nazumuddin
[2]Assistant Professor [2]Head Of the Department, [3]Post Graduate Student, [3]Assistant Professor
Dept. of Aerospace Engg., Nimra Institute Of Science And Technology, Ibrahimpatnam-521456, India.

***Abstract* - Design and analysis of propellant grain configurations for determination of the grain geometry which is an important and critical step in the design of solid propellant rocket motors, because accurate calculation of grain geometrical properties plays a vital role in performance prediction. The performance prediction of the solid rocket motor can be achieved easily if the burn back steps of the grain are known. In this study, grain burn back analysis for 3-D star grain geometries for solid rocket motor was investigated. The design process involves parametric modeling of the geometry in CATIA software through dynamic variables that define the complex configuration. Initial geometry is defined in the form of a surface which defines the grain configuration. Grain burn back is achieved by making new surfaces at each web increment and calculating geometrical properties at each step. Equilibrium pressure method is used to calculate the internal ballistics. The procedure adopted can be applied to any complex geometry in a relatively simple way for preliminary designing of grain configuration. As the propellant in the igniter burns which would reduce the area of the remaining propellant and by which there will be an change of pressure in the Solid Rocket Motor with respect to the time and this change in the pressure with cause variation in mass flow rate and in this paper the variation of the thrust with respect to the time is calculated .The areas of the grain are found by using MATLAB using 0.05 mm half set and which is gives the area of the remaining grain in the Solid Rocket Motor. The numerical results from the CATIA are checked with the MATLAB and to verify the correct area of the remaining propellant.**

***Key words* - Computer aided design, Computer-aided three-dimensional interactive application, Matrix laboratory, Solid rocket propulsion–geometry optimizer, System analysis ram transport.**

Nomenclature used:

1. **CAD - Computer Aided Design**
2. **CATIA-Computer-Aided Three-Dimensional Interactive Application**
3. **MATLAB- Matrix Laboratory**
4. **mm - Milli meters**
5. **N/mm^2 - Newton per square millimeter**

I. INRODUCTION

Initial phase of solid propellant rocket motor development is characterized with number of parametric studies undertaken in order for rocket mission to be accomplished. During the process of assessment of possible solutions for propellant charge shape, configuration of motor and type of propellant charge, problems of production are being considered, demands for specific motor performances and conditions of exploitations. Even though these preliminary project studies are comprehensive, from practical side, it is not good practice to treat all the influencing factors parametrically. Instead, after first assessment of possible solutions, optimal construction is chosen.

It is then further subjected to detail analysis. Using this analysis, following is critically tested: propellant type – geometry of propellant grain – motor structure, in order to determine whether the motor will satisfy parameters necessary for of solid propellant rocket motor design. One of the main objective for designers of solid propellant rocket motor is defining propellant grain which will enable required change of thrust vs. time, needed for fulfillment of rocket mission, taking care of other specific limitations (envelope, mass, etc.). Analysis of solid propellant rocket motors is progressing in two levels, where, independent of level, it is needed to assess following four basic steps.

The steps are, Assessment of several types of propellant types/configurations, Defining the geometry of propellant grain which satisfies conditions of internal ballistics and structural integrity, Approximate determination of erosive burning and potential instability of burning process, Determination of structural integrity of the grain during time of pressure increase during ignition.

First level or preliminary analysis of design uses tools that have to be simple and adaptable to user. There are usually simple computer codes, based on analytical models or diagrams that give simple first results.

Second level is level of final design of propellant charge. Tools for this task are more refined and these are handled by experts for propellant grain design. Computer codes are based on finite difference methods or finite element methods, with 1D, 2D or 3D models of physical phenomena (internal ballistics, fluid dynamics, continuum mechanics structural analysis). They allow precise calculations, or optimization up to defining final geometry.

Countries with high technological level focus their continual research on prediction of theoretical performances of solid propellant rocket motor. They base their research on development of high range ballistic guided rockets, based on composite propellant charges. Large number of experimental research, conducted during the development of these rocket systems, enabled huge database of influencing factors on dispersion of real from ideal performances of rocket motor, for every system individually.

Every weapon requires some type of propulsion to deliver its warhead to the intended target. This chapter will be a study of the propulsion systems used to propel weapons to their targets and the design requirements for the vehicles themselves. The underlying principle of propulsive movement has been stated by Newton in his Third Law of Motion: To every action there is an equal and opposite reaction. Every forward acceleration or charge in motion is a result of a reactive force acting in the opposing direction. A person walks forward by pushing backwards against the ground. In a propeller-type airplane, the air through which it is moving is driven backward to move the airplane forward. In a jet-propelled plane or a rocket, a mass of gas is emitted rearward at high speed, and the forward motion of the plane is a reaction to the motion of the gas. Matter in the form of a liquid, a gas, or a solid may be discharged as a propellant force, expending its energy in a direction opposite to the desired path of motion, resulting in a predetermined acceleration of the propelled body along a desired trajectory.

Solid propellants are used in forms called grains. A grain is any individual particle of propellant regardless of the size or shape. The shape and size of a propellant grain determines the burn time, amount of gas, and rate produced from the burning propellant and, as a consequence, thrust vs. time profile. Burn rate is one of two major variables of the mass flow, yet many factors the burn rate itself. Composition of the propellant plays a major role but is predetermined. Moreover the composition is usually the same throughout the entire propellant mass. Experimentally determining the properties of the propellant composition we can leave out much of its properties as they will not have an effect on variable performance. Therefore if the other effecting factors are negligible the burn rate is very predictable. The conditions affecting the burn rate are: First and foremost the pressure in the combustion chamber, Initial temperature of the propellant.

II. EXPERIMENTAL DETAILS

A. Design Methodology

The primary objective of design is Defining propellant grain which will enable required change of thrust vs. time, needed for fulfillment of rocket mission, taking care of other specific limitations (envelope, mass, etc.). Analysis of solid propellant rocket motors is progressing in two levels, where, independent of level, it is needed to assess following four basic steps

- Assessment of several types of propellant types/configurations,
- Defining the geometry of propellant grain which satisfies conditions of internal ballistics and structural integrity,
- Approximate determination of erosive burning and potential instability of burning process,
- Determination of structural integrity of the grain during time of pressure increase during ignition.

First level or preliminary analysis of design uses tools that have to be simple and adaptable to user. There are usually simple computer codes, based on analytical models or diagrams that give simple first results.

Second level is level of final design of propellant charge. Tools for this task are more refined and these are handled by experts for propellant grain design. Computer codes are based on finite difference methods or finite element methods, with 1D, 2D or 3D models of physical phenomena (internal ballistics, fluid dynamics, continuum mechanics structural analysis). They allow precise calculations, or optimization up to defining final geometry.

B. Problem Definition

Design and analysis of propellant grain configurations for determination of the grain geometry which is an important and critical step in the design of solid propellant rocket motors, because accurate calculation of grain geometrical properties plays a vital role in performance prediction. The performance prediction of the solid rocket motor can be achieved easily if the burn back steps of the grain are known. In this study, grain burn back analysis for 3-D star grain geometries for solid rocket motor was investigated

C. Design and Analysis

CATIA(Computer Aided Three-dimensional Interactive Application)

CATIA is the leading product development solution for all manufacturing organizations, from OEMs, through their supply chains, to small independent producers. The range of CATIA capabilities allows it to be applied in a wide variety of industries, such as aerospace, automotive, industrial machinery, electrical, electronics, shipbuilding, plant design, and consumer goods, including design for such diverse products as jewelry and clothing.

CATIA is the only solution capable of addressing the complete product development process, from product concept specification through product-in-service, in a fully integrated and associative manner. Based on an open, scalable architecture, it facilitates true collaborative engineering across the multidisciplinary extended enterprise, including style and form design, mechanical design and equipment and systems engineering, managing digital mock-ups, machining, analysis, and simulation. By enabling enterprises to reuse product design knowledge and accelerate development cycles, CATIA helps companies to speed-up their responses to market needs. Commonly referred to as a 3D Product Lifecycle Management software suite, CATIA supports multiple stages of product development (CAx), including conceptualization, design (CAD), manufacturing (CAM), and engineering (CAE).

CATIA facilitates collaborative engineering across disciplines, including surfacing & shape design, mechanical engineering, and equipment and systems engineering. CATIA provides a suite of surfacing, reverse engineering, and visualization solutions to create, modify, and validate complex innovative shapes, from subdivision, styling, and Class A surfaces to mechanical functional surfaces.

CATIA enables the creation of 3D parts, from 3D sketches, sheet metal, composites, molded, forged or tooling parts up to the definition of mechanical assemblies. It provides tools to complete product definition, including functional tolerances as well as kinematics definition.

In this project, grain burn back analysis for 3-d star grain geometries for solid rocket motor was investigated. The design process involves parametric modeling of the geometry in CATIA software through dynamic variables that define the complex configuration. Initial geometry is defined in the form of a surface which defines the grain configuration. Grain burn back is achieved by making new surfaces at each web increment and calculating geometrical properties at each step. Equilibrium pressure method is used to calculate the internal ballistics. The procedure adopted can be applied to any complex geometry in a relatively simple way for preliminary designing of grain configuration.

The areas of the grain are found by using CATIA v5 using 1mm half set and which is gives the area of the remaining grain in the igniter. The numerical results from the CATIA are compared with the MATLAB and correct area of the remaining propellant is verified.

MATLAB (Matrix Laboratory)

MATLAB is a multi-paradigm numerical computing environment and fourth-generation programming language. Developed by Math Works, MATLAB allows matrix manipulations, plotting of functions and data, implementation of algorithms, creation of user interfaces, and interfacing with programs written in other languages, including C, C++, Java, and Fortran. Although MATLAB is intended primarily for numerical computing, an optional toolbox uses the MuPAD symbolic engine, allowing access to symbolic computing capabilities.

An additional package, Simulink, adds graphical multi-domain simulation and Model-Based Design for dynamic and embedded systems.

In 2004, MATLAB had around one million users across industry and academia. MATLAB users come from various backgrounds of engineering, science, and economics. MATLAB is widely used in academic and research institutions as well as industrial enterprises.

Fig..1 CATIA Model Star Grain

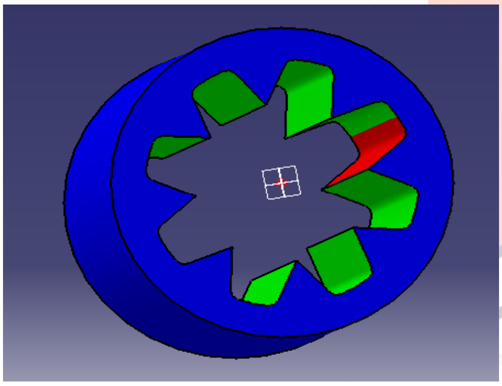

Fig..2 Repeated shape for Star Grain

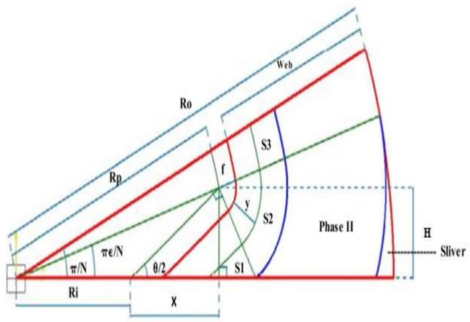

Calculation for H ,

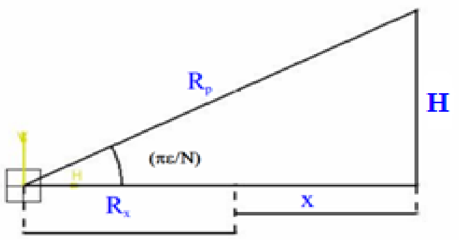

$$\text{Sin}\left(\frac{\pi\varepsilon}{N}\right) = \left(\frac{H}{R_p}\right)$$

$$\text{H} = R_p\ \text{Sin}\left(\frac{\pi\varepsilon}{N}\right)$$

$$\text{Tan}\left(\frac{\pi\varepsilon}{N}\right) = \left(\frac{H}{x + Ri}\right)$$

$$\text{H} = (x + R_i)\ \text{Tan}\left(\frac{\pi\varepsilon}{N}\right)$$

From 1 and 2

$$R_p\ \text{Sin}\left(\frac{\pi\varepsilon}{N}\right) = (x + R_i)\ \text{Tan}\left(\frac{\pi\varepsilon}{N}\right)$$

$$\left[\frac{R_p\ Sin\left(\frac{\pi\varepsilon}{N}\right)}{Tan\left(\frac{\pi\varepsilon}{N}\right)}\right] - R_i = x$$

$$\text{Tan}\left(\frac{\theta}{2}\right) = \left(\frac{H}{x}\right)$$

From above equations

$$\text{Tan}\left(\frac{\theta}{2}\right) = \left[\frac{R_p\ Sin\left(\frac{\pi\varepsilon}{N}\right)Tan\left(\frac{\pi\varepsilon}{N}\right)}{R_p\ Sin\left(\frac{\pi\varepsilon}{N}\right) - R_i Tan\left(\frac{\pi\varepsilon}{N}\right)}\right]$$

$$\left(\frac{\theta}{2}\right) = Tan^{-1}\left[\frac{R_p\ Sin\left(\frac{\pi\varepsilon}{N}\right)Tan\left(\frac{\pi\varepsilon}{N}\right)}{R_p\ Sin\left(\frac{\pi\varepsilon}{N}\right) - R_i Tan\left(\frac{\pi\varepsilon}{N}\right)}\right]$$

$$\theta = 2\,Tan^{-1}\left[\frac{R_p\ Sin\left(\frac{\pi\varepsilon}{N}\right)Tan\left(\frac{\pi\varepsilon}{N}\right)}{R_p\ Sin\left(\frac{\pi\varepsilon}{N}\right) - R_i Tan\left(\frac{\pi\varepsilon}{N}\right)}\right]$$

Phase I ,
Calculation for S_1 ,

$$\text{Sin}\left(\frac{\pi\varepsilon}{N}\right) = \frac{H}{R_p}$$

$$R_p\ \text{Sin}\left(\frac{\pi\varepsilon}{N}\right) = H$$

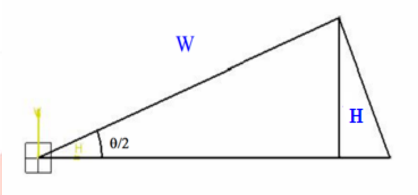

$$Sin\left(\frac{\theta}{2}\right) = \frac{H}{w}$$

$$H = w\,Sin\left(\frac{\theta}{2}\right)$$

From 1 and 6

$$\text{R}_p\ \text{Sin}\left(\frac{\pi\varepsilon}{N}\right) = \left[w\,Sin\left(\frac{\theta}{2}\right)\right]$$

$$w = \left[\frac{R_p\ Sin\left(\frac{\pi\varepsilon}{N}\right)}{Sin\left(\frac{\theta}{2}\right)}\right]$$

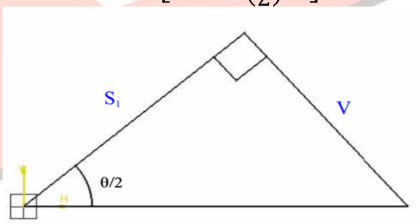

$$tan\left(\frac{\theta}{2}\right) = \frac{v}{S_1}$$

$$v = S_1 tan\left(\frac{\theta}{2}\right)$$

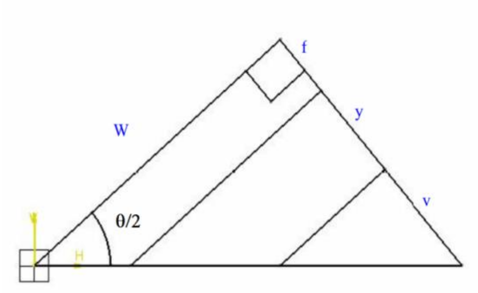

$$cot\left(\frac{\theta}{2}\right) = \left(\frac{w}{f + y + v}\right)$$

$$w = (f + y + v)\,cot\left(\frac{\theta}{2}\right)$$

$$w = \left[f + y + S_1\,tan\left(\frac{\theta}{2}\right)\right]\ cot\left(\frac{\theta}{2}\right)$$

$$w = (f + y)\,cot\left(\frac{\theta}{2}\right) + S_1$$

$$S_1 = w - (f + y)\cot\left(\frac{\theta}{2}\right)$$

$$S_1 = \left[\frac{R_p\ Sin\left(\frac{\pi\varepsilon}{N}\right)}{sin\left(\frac{\theta}{2}\right)}\right] - \left[(f + y)\cot\left(\frac{\theta}{2}\right)\right]$$

Calculation for S_2 ,

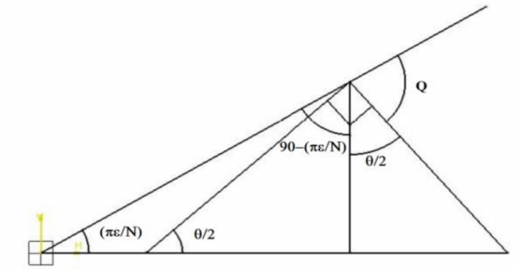

$$Q = \pi - \left[\left(\frac{\pi}{2}\right) - \left(\frac{\pi\varepsilon}{N}\right)\right] - \left(\frac{\theta}{2}\right)$$

$$Q = \left(\frac{\pi}{2}\right) - \left(\frac{\theta}{2}\right) + \left(\frac{\pi\varepsilon}{N}\right)$$

$$S_2 = (y + f)Q$$

$$S_2 = \left\{(y + f)\left[\left(\frac{\pi}{2}\right) - \left(\frac{\theta}{2}\right) + \left(\frac{\pi\varepsilon}{N}\right)\right]\right\}$$

Calculation for S_3 ,

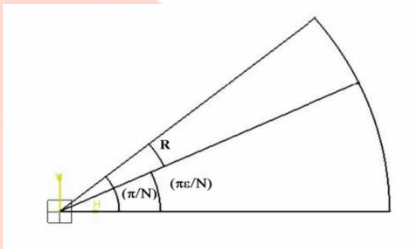

$$R = \left(\frac{\pi}{N}\right) - \left(\frac{\pi\varepsilon}{N}\right)$$

$$S_3 = \left\{(R_p + y + f)\left[\left(\frac{\pi}{N}\right) - \left(\frac{\pi\varepsilon}{N}\right)\right]\right\}$$

Perimeter ,

$$S_p = 2N(S_1 + S_2 + S_3)$$

$$S_p = 2N\left\{\left[\frac{R_p\ Sin\left(\frac{\pi\varepsilon}{N}\right)}{sin\left(\frac{\theta}{2}\right)} - (y + f)\cot\left(\frac{\theta}{2}\right)\right] + \left[(y + f)\left[\left(\frac{\pi}{2}\right) - \left(\frac{\theta}{2}\right) + \left(\frac{\pi\varepsilon}{N}\right)\right]\right] + \left[(R_p + y + f)\left(\left(\frac{\pi}{N}\right) - \left(\frac{\pi\varepsilon}{N}\right)\right)\right]\right\}$$

Burn surface area ,

$$A_s = S_p\ L \quad [L = length\ of\ grain]$$

Port area ,

$$A_p = 2N\left\{\frac{1}{2}R_p \sin\left(\frac{\pi\varepsilon}{N}\right)\left[R_p\cos\left(\frac{\pi\varepsilon}{N}\right) + R_p\sin\left(\frac{\pi\varepsilon}{N}\right)\tan\left(\frac{\theta}{2}\right)\right] - \frac{1}{2}\left[\frac{R_p\sin\left(\frac{\pi\varepsilon}{N}\right)}{\sin\left(\frac{\theta}{2}\right)} - (y + f)\cot\left(\frac{\theta}{2}\right)\right]^2 \tan\left(\frac{\theta}{2}\right) + \frac{1}{2}(y + f)^2\left[\frac{\pi}{2} - \frac{\theta}{2} + \frac{\pi\varepsilon}{N}\right] + \frac{1}{2}(R_p + f + y)^2\left[\frac{\pi}{N} - \frac{\pi\varepsilon}{N}\right]\right\}$$

Port volume ,$V_p = A_p * L \quad [L = length\ of\ grain]$

Phase II ,

$$S_1 = \left[\frac{R_p\ Sin\left(\frac{\pi\varepsilon}{N}\right)}{sin\left(\frac{\theta}{2}\right)}\right] - (f + y)\cot\left(\frac{\theta}{2}\right)$$

As exceeding to phase ‖ , then $S_1 = 0$

$$0 = \left[\frac{R_p\ Sin\left(\frac{\pi\varepsilon}{N}\right)}{sin\left(\frac{\theta}{2}\right)}\right] - (f + y)\cot\left(\frac{\theta}{2}\right)$$

$$(f + y)\cot\left(\frac{\theta}{2}\right) = \left[\frac{R_p\ Sin\left(\frac{\pi\varepsilon}{N}\right)}{sin\left(\frac{\theta}{2}\right)}\right]$$

$$y = \left[\frac{R_p \sin\left(\frac{\theta}{2}\right)}{\cos\left(\frac{\theta}{2}\right)}\right] - f$$

Now there is no S_1. Only S_2 & S_3

S_2 = Angle $(f + y)$

S_3 = Won't change = $\left[(R_p + y + f)\left(\left(\frac{\pi}{N}\right) - \left(\frac{\pi\varepsilon}{N}\right)\right)\right]$

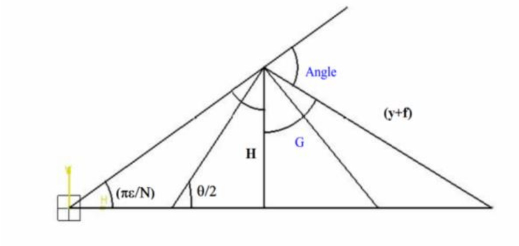

$$\text{Tan G} = \frac{\sqrt{(f+y)^2 - {H_1}^2}}{H_1}$$

$$\text{G} = Tan^{-1}\left(\frac{\sqrt{(f+y)^2 - {H_1}^2}}{H_1}\right)$$

$$\text{Angle} = \pi - \text{G} - \left(\frac{\pi}{2} - \frac{\pi\varepsilon}{N}\right) = \frac{\pi}{2} - Tan^{-1}\left(\frac{\sqrt{(f+y)^2 - {H_1}^2}}{H_1}\right) + \frac{\pi\varepsilon}{2}$$

$$\text{Angle} = \frac{\pi}{2} + \frac{\pi\varepsilon}{N} - Tan^{-1}\left(\frac{\sqrt{(f+y)^2 - {H_1}^2}}{H_1}\right)$$

$$S_2 = \left\{\frac{\pi}{2} + \frac{\pi\varepsilon}{N} - Tan^{-1}\left(\frac{\sqrt{(f+y)^2 - {H_1}^2}}{H_1}\right)\right\}(y + f)$$

Now ,
Perimeter ,

$$S_p = 2\text{N}\,[\,S_2 + S_3]$$

$$S_p = 2\text{N}\left\{\left[\frac{\pi}{2} + \frac{\pi\varepsilon}{N} - Tan^{-1}\left(\frac{\sqrt{(f+y)^2 - {H_1}^2}}{H_1}\right)\right](y + f) + \left[(R_p + y + f)\left(\left(\frac{\pi}{N}\right) - \left(\frac{\pi\varepsilon}{N}\right)\right)\right]\right\}$$

Burn surface area ,

$$A_s = S_p\ L$$

Port area ,

$$A_p = 2N\left\{\frac{1}{2}\left\{\frac{\pi}{2} + \frac{\pi\varepsilon}{N} - Tan^{-1}\left(\frac{\sqrt{(f+y)^2 - {H_1}^2}}{H_1}\right)\right\}(y + f)^2 + \frac{1}{2}\text{Cot}\left(\frac{\pi\varepsilon}{\text{N}}\right)\text{H}^2 + \frac{1}{2}\text{H}\sqrt{(\text{y}+\text{f})^2 - \text{H}^2} + \frac{1}{2}(R_p + f + y)^2\left[\frac{\pi}{N} - \frac{\pi\varepsilon}{N}\right]\right\}$$

(4.27)

Port volume ,

$$V_p = A_p\ L$$

Phase III,
There will be only S_3

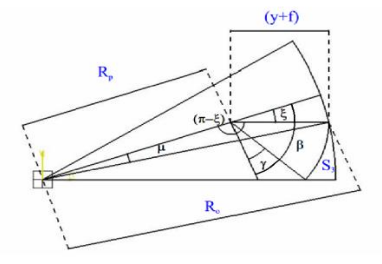

$$\beta = \left(\frac{\pi}{2} - \frac{\theta}{2} + \frac{\pi\varepsilon}{N}\right)$$

$$\text{Tan}\left(\frac{\theta}{2} + \gamma\right) = \left(\frac{\sqrt{(f+y)^2 - {R_p}^2 Sin^2\left(\frac{\pi\varepsilon}{N}\right)}}{R_p\ Sin\left(\frac{\pi\varepsilon}{N}\right)}\right)$$

$$\frac{\theta}{2} + \gamma = Tan^{-1}\left(\frac{\sqrt{(f+y)^2 - {R_p}^2 Sin^2\left(\frac{\pi\varepsilon}{N}\right)}}{R_p\ Sin\left(\frac{\pi\varepsilon}{N}\right)}\right)$$

$$\gamma = Tan^{-1}\left(\frac{\sqrt{(f+y)^2 - {R_p}^2 Sin^2\left(\frac{\pi\varepsilon}{N}\right)}}{R_p\ Sin\left(\frac{\pi\varepsilon}{N}\right)}\right) - \frac{\theta}{2}$$

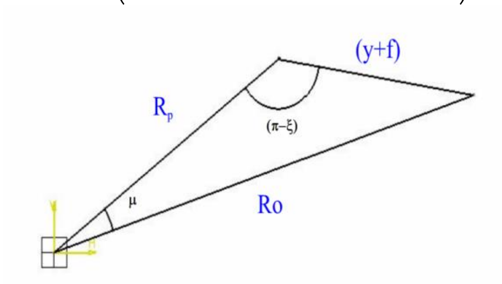

Cosine law ,

$$ {R_0}^2 = (y+f)^2 + {R_p}^2 - 2R_p(y+f)\,Cos\,(\pi - \xi)$$

$$Cos\,(\pi - \xi) = -\frac{{R_0}^2 - {R_p}^2 - (y+f)^2}{2R_p(y+f)}$$

$$\xi = \pi - Cos^{-1}\left(-\frac{{R_0}^2 - {R_p}^2 - (y+f)^2}{2R_p(y+f)}\right)$$

Perimeter ,

$$S = 2N\,(S_3)$$

$$S = 2N\big((y+f)(\beta - \gamma - \xi)\big)$$

$$S = 2N\left[(y+f)\left(\left(\frac{\pi}{2} - \frac{\theta}{2} + \frac{\pi\varepsilon}{N}\right) - Tan^{-1}\left(\frac{\sqrt{(f+y)^2 - {R_p}^2 Sin^2\left(\frac{\pi\varepsilon}{N}\right)}}{R_p\ Sin\left(\frac{\pi\varepsilon}{N}\right)}\right) + \frac{\theta}{2} - \pi - Cos^{-1}\left(-\frac{{R_0}^2 - {R_p}^2 - (y+f)^2}{2R_p(y+f)}\right)\right)\right]$$

Burn surface area ,

$$A_p = S_p\,L$$

$$(y_{max} + f)^2 = \left(R_0 - R_p\,Cos\left(\frac{\pi\varepsilon}{N}\right)\right)^2 + \left(R_p\,Sin\left(\frac{\pi\varepsilon}{N}\right)\right)^2$$

$$y_{max} = \sqrt{\left(R_0 - R_p\,Cos\left(\frac{\pi\varepsilon}{N}\right)\right)^2 + \left(R_p\,Sin\left(\frac{\pi\varepsilon}{N}\right)\right)^2} - f$$

From sine law ,

$$\frac{R_p}{Sin\,(\pi - \xi)} = \frac{y+f}{Sin\,\mu}$$

$$\mu = Sin^{-1}\left(\frac{(y+f)}{R_o}\,Sin\,(\pi - \xi)\right)$$

$$A_p = N\left({R_p}^2\left(\frac{\pi}{N}(1-\varepsilon) + \mu\right) + (f+y)^2(\beta - \gamma - \xi) + R_p Sin\left(\frac{\pi\varepsilon}{N}\right)\left(R_p Cos\left(\frac{\pi\varepsilon}{N}\right) + \sqrt{(f+y)^2 - {R_p}^2 Sin^2\left(\frac{\pi\varepsilon}{N}\right)}\right) - R_p Sin\,\mu\left(R_p Cos\,\mu + \sqrt{(f+y)^2 - {R_p}^2 Sin^2\mu}\right)\right)$$

Port volume ,

$$V_p = A_p\,L$$

D. Programming

MATLAB PROGRAM FOR STAR GRAIN

```
clear all;
clc;

%*********************************************************************
%PROGRAM FOR THRUST VS TIME GRAPH OF STAR GRAIN
%*********************************************************************

%INPUT PERAMETERS
```

```
nsp=input('ENTER THE NO. OF STAR POINTS:')
w=input('ENTER THE WEB THICKNESS (mm):')
ro=input('ENTER THE OUTER RADIUS (mm):')
%ri=input('ENTER THE INNER RADIUS:')
OA=input('ENTER THE OPENING ANGLE IN DEGREES:')
ef=input('ENTER THE ANGULAR FRACTON:')
f=input('ENTER THE FILLET RADIUS (mm):')
L=input('ENTER THE LENGTH OF GRAIN (mm)')
rin=input('ENTER THE INITIAL BURN RATE(mm/sec)')
pin=input('ENTER THE INITIAL PRESSURE (N/mm2)')
n=input('ENTER THE CONSTANT INPUT VALUE FOR n')
d=input('ENTER THE DENSITY OF CHAMBER (kg/mm3)')
v=input('ENTER THE CHARECTERISTIC VELOCITY (mm/sec)')
D=input('ENTER THE THROAT DIAMETER (mm)')
x=input('ENTER THE EACH EXTENT VALUE FOR WHICH PROGRAM WRITTEN (mm)')

%CALCULATION FOR CONSTANT VALUES

At=4*(pi/4)*(D^2);
a=(rin/((pin)^n));
rp=ro-w-f;
H=rp*sin(pi*ef/nsp);
%OA=2*atan(rp*sin(pi*ef/nsp)*tan(pi*ef/nsp)/(rp*sin(pi*ef/nsp)-ri*tan(pi*ef/nsp)));
oa=OA*pi/180;
is=0;
ymax=sqrt(((ro-rp*cos(pi*ef/nsp))^2)+(rp*sin(pi*ef/nsp))^2)-f;
ym=ymax-abs((ymax-round(ymax)));
B=((pi/2)-(oa/2)+(pi*ef/nsp));

%CALCULATION FOR VARIBLE VALUES

for y=0:0.05:(rp*(sin(ef*pi/nsp)/cos(oa/2)))-f;

    is=is+1;
    t(1)=0;
    p(1)=0;

    %CONDITIONS FOR PHASE I

  if (y<=(rp*(sin(ef*pi/nsp)/cos(oa/2)))-f)

      s1=(rp*sin(pi*ef/nsp)/sin(oa/2))-((y+f)*cot(oa/2));
      s2=(y+f)*((pi/2)-(oa/2)+(pi*ef/nsp));
      s3=(rp+y+f)*((pi/nsp)-(pi*ef/nsp));
      s=(2*nsp)*(s1+s2+s3);
      A=s*L;
      p(is+1)=((a*A*d*v/At)^(1/(1-n)));
      T(is+1)=(p(is+1)*At);

  end

  r(is)=a*(p(is+1)^n);
  dt(is)=(x/r(is));
  t(is+1)=t(is)+dt(is);

end

for y=(rp*(sin(ef*pi/nsp)/cos(oa/2)))-f:0.05:w;

    is=is+1;

    %CONDITIONS FOR PHASE II
```

```
  if (((rp*(sin(ef*pi/nsp)/cos(oa/2)))-f)<y<=w)

    s=(2*nsp)*((y+f)*((pi*ef/nsp)+(pi/2)-(atan((sqrt(((y+f)^2)-(H^2)))/H)))+((rp+y+f)*((pi/nsp)-(pi*ef/nsp))));
    A=s*L;
    p(is+1)=((a*A*d*v/At)^(1/(1-n)));
    T(is+1)=(p(is+1)*At);

  end

  r(is)=a*(p(is+1)^n);
  dt(is)=(x/r(is));
  t(is+1)=t(is)+dt(is);

end

for y=w:0.05:ym;

   is=is+1;

   %CONDITIONS FOR PHASE III

  if (w<y<=ym)

    G=(atan(sqrt(((y+f)^2)-((rp*sin(ef*pi/nsp))^2))/(rp*sin(pi*ef/nsp))))-(oa/2);
    Z=(pi)-(acos(-((ro^2)-(rp^2)-((y+f)^2))/(2*rp*(y+f))));
    s=(2*nsp)*((y+f)*(B-G-Z));
    A=s*L;
    p(is+1)=((a*A*d*v/At)^(1/(1-n)));
    T(is+1)=(p(is+1)*At);

  end

  r(is)=a*(p(is+1)^n);
  dt(is)=(x/r(is));
  t(is+1)=t(is)+dt(is);

end

%CONDTION TO PLOT GRAPH FOR THRUST VS TIME

plot(t,T)
```

Note: Similarly the design and Analysis done for Truncated star, dog-bone and Dendrite shapes, and results obtained.

III. RESULTS & DISCUSSION

Table 1 Parameter inputs of Star Grain

S.No	Input Parameters	Representation	Values
1	Number of star points	N	8
2	Web thickness (mm)	w	10
3	Outer radius (mm)	R_o	50
4	Inner radius(mm)	R_i	-
5	Opening angle in degrees	θ	74
6	Angular fraction	ε	0.7
7	Fillet radius (mm)	f	3
8	Length of grain (mm)	L	520
9	Initial burn rate(mm/sec)	r	8
10	Initial pressure (n/mm2)	P_o	0.4
11	Constant input value for n	n	0.334
12	Density of chamber (kg/mm^3)	ρ	1700
13	Characteristic velocity (mm/sec)	v	1500000
14	Throat diameter (mm)	D	13
15	The each extent value for which program	x	0.05

	written (mm)		

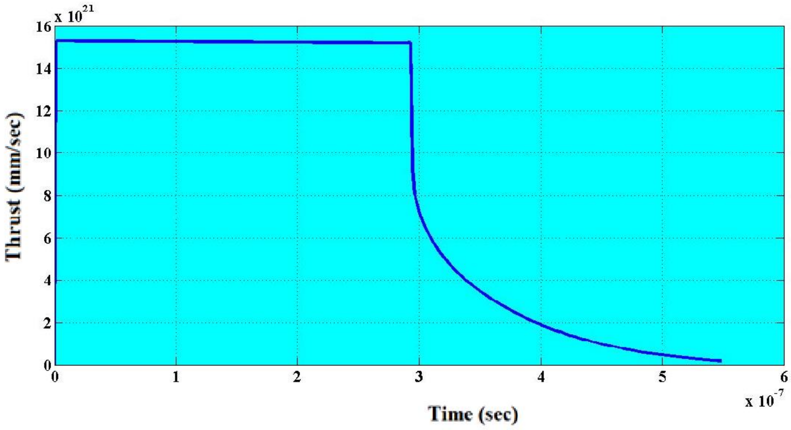

Graph 1: Thrust Vs Time graph for Star Grain

For star grain shape we got neutral burn, that means constant thrust with respect to time until the total propellant burns in the solid rocket motor. It is very useful in case of igniters of pyrogen which we are using for ignition of large solid rocket motors.

We got regressive burn for truncated star, neutral burn for wagon wheel, somewhat neutral and a slight progressive for dog bone and totally a different profile for dendrite that sudden decent and constant neutral burn until total propellant burns.

That means the other grain shapes are not so continuous thrust with respect to time but they can use in their aspect of mission requirement.

In this way can calculate Thrust Vs Time graphs for different grain shapes. The procedure follows the same thing. The only thing is design of mission, for which can calculate more efficient grain shape.

IV. CONCLUSION

1. Prediction of pressure while burning the grain is more important ballistic parameter to find the thrust and mass flow rate of hot gasses throughout the burning of rocket motor.
2. The burn surface area and burn rate of the grain will dictate the variation of pressure during propellant burning inside the chamber
3. This burn rate variation is not possible to measure exact values. However we have tried to get burn surface area at an increment of 1 mm till the completion of web thickness and 0.1 mm during sliver burning.
4. To estimate this burn surface area we have used increment method by using CATIA application software , and cross checked with the MATLAB 7 software program.

Based on burn surface area, we have predicted the corresponding variation of pressure and mass flow rate in the chamber with respect to time

REFERENCES

[1] Abramson, M.A. et al.: OrthoMADS: A deterministic MADS instance with orthogonal directions.
[2] SIAM Journal on Optimization, Volume 20, Issue 2, Pages 948-966, 2009.
[3] Acik, S.: Internal Ballistic Design Optimization of a Solid Rock et Motor. Department of Mechanical Engineering, Middle East Technical University, 2010.
[4] Anon.: IMSL: Fortran Subroutines for Mathematical Applications Vol. 2, Visual Numerics, Inc. 1997.
[5] Antonov, A.: Solid Rocket Motors Performance and Grain Geometry Optimization. SART TN-003/2011, German Aerospace Center, Bremen, Germany, 2011.
[6] Audet, C., Dennis Jr., J.E.: Mesh Adaptive Direct Search Algorithms for Constrained Optimization. SIAM Journal on Optimization, Volume 18, Issue 1, Pages 188-217, 2006.
[7] Bairstow, B.K.: Effectiveness of Integration of System-Level Optimization in Concurrent Engineering for Rocket Design. Department of Aeronautics and Astronautics, Massachusetts Institute of Technology, 2006.
[8] Braeunig, R.A.: Rocket Propulsion. Available at: http://www.braeuning.us/space/propuls.htm, 2009, accessed 22nd January 2012.
[9] Berghen, F.V, Bersini, H.: CONDOR, a New Parallel, Constrained Extension of Powell's UOBYQA Algorithm: Experimental Results and Comparison with the DFO Algorithm. Journal of Computational and Applied Mathematics, Volume 181, Issue 1, Pages 157-175, 2005.
[10] Booker, A.J. et al.: A Rigorous Framework for Optimization of Expensive Functions by Surrogates. Structural and Multidisciplinary Optimization, Volume 17, Issue 1, Pages 1-13, 1999.
[11] Brooks, W.T., Keller Jr., R.B. ed.: Solid Propellant Grain Design and Internal Ballistics. SP-8076, NASA, 1972.
[12] Csendes, T. et al.: The GLOBAL Optimization Method Revisited. Optimization Letters, Volume 2, Issue 4, Pages 445-454, August 2008.
[13] Chang, Kenneth. "NASA Tests Engine With an Uncertain Future". New York Times(August 30, 2010). Retrieved 2010-08-31.
[14] David K. Stumpf. Titian II: A History of a Cold War Missile Program. University of Arkansas Press. ISBN 1-55728-601-9(2000).

[15] Davidson, W.C.: Variable Metric Method for Minimization. SIAM Journal on Optimization, Volume 1, Issue 1, Pages 1-17, 1991.

[16] Del Rio, M.S.: Xop/Xplot User's Guide. Available at http://ftp.esrf.eu/pub/scisoft/xop2.0/ XopTutorial/XplotManual.pdf, 2001, accessed 14 Mars 2012.

[17] Dexter K Huzel and David H. Huang, NASA SP-125, Design of Liquid Propellant Rocket Engines Second edition of a technical report obtained from the website of the National Aeronautics and Space Administration (NASA) (1971).

[18] Digabel, S.L.: Algorithm 909: NOMAD: Nonlinear optimization with the MADS algorithm. ACM Transactions on Mathematical Software, Volume 37, Issue 4, Pages 44-59, 2011.

[19] Dumont, E., Kopp, A., Sippel, M.: SRP 1.2: Updates and Simulation Results . SART TN013/2009, German Aerospace Center, Bremen, Germany, 2009.

[20] E. C. Fernandes and M. V. Heitor, "Unsteady flames and the Rayleigh criterion" in F. Culick, M. V. Heitor, and J. H. Whitelaw (Editors). Unsteady Combustion (1st ed.). Kluwer Academic Publishers. p. 4. ISBN 0-7923-3888-X(1996).

[21] George P. Sutton and Oscar Biblarz. Rocket Propulsion Elements (7th ed.). Wiley Interscience(2001). ISBN 0-471-32642-9.

[22] Haidn, O.J.: Advanced Rock et Engines. RTO-EN-AVT-150, Advances on Propulsion Technology for High-Speed Aircraft, Rhode St. Genèse, Belgium, 2007.

[23] Hansen, P., Mladenović, N.: Variable neighborhood search: Principles and applications.

[24] European Journal of Operational Research, Volume 130, Issue 3, Pages 449-467, 2001.

[25] Hartfield, R. et al.: A Review of Analytical Methods for Solid Rock et Motor Grain Analysis. AIAA 2003-4506, 39th Joint Propulsion Conference and Exhibit, Huntsville, USA, 2003.

[26] Johnson, S.G.: The NLopt nonlinear-optimization pack age. Available at: http://ab-initio .mit.edu/ nlopt, 2008, accessed 25 January 2012.